Quaternary Research 71 (2009) 385–396

Contents lists available at ScienceDirect

Quaternary Research

journal homepage: www.elsevier.com/locate/yqres

# Last glacial fire regime variability in western France inferred from microcharcoal preserved in core MD04-2845, Bay of Biscay

Anne-Laure Daniau [a,b,*], Maria Fernanda Sánchez Goñi [a], Josette Duprat [a]

[a] Université de Bordeaux1, EPHE, CNRS UMR5805, EPOC, bât B18, Avenue des Facultés, 33405 TALENCE Cedex, France
[b] Université de Bordeaux1, CNRS UMR5199 PACEA, Institut de Préhistoire et Géologie du Quaternaire, bât B18, Avenue des Facultés, 33405 TALENCE Cedex, France

ARTICLE INFO

*Article history:*
Received 17 January 2008
Available online 19 March 2009

*Keywords:*
Marine sequence
Charcoal
Biomass burning
France
Dansgaard–Oeschger events
Heinrich events

ABSTRACT

High resolution multiproxy analysis (microcharcoal, pollen, organic carbon, *Neogloboquadrina pachyderma (s)*, ice rafted debris) of the deep-sea record MD04-2845 (Bay of Biscay) provides new insights for understanding mechanisms of fire regime variability of the last glacial period in western France. Fire regime of western France closely follows Dansgaard–Oeschger climatic variability and presents the same pattern than that of southwestern Iberia, namely low fire regime associated with open vegetation during stadials including Heinrich events, and high fire regime associated with open forest during interstadials. This supports a regional climatic control on fire regime for western Europe through fuel availability for the last glacial period. Additionally, each of Heinrich events 6, 5 and 4 is characterised by three episodes of fire regime, with a high regime bracketed by lower fire regime episodes, related to vegetational succession and complex environmental condition changes.



## Introduction

Beyond man-made fires, biomass burning depends on climate and also appears to be a significant driver for climate change through the release of greenhouse gases, namely carbon dioxide, methane, nitric oxide and aerosols (Crutzen et al., 1979; Lobert et al., 1990; Andreae and Merlet, 2001; van Aardenne et al., 2001; Van der Werf et al., 2004; Thonicke et al., 2005). Variations of atmospheric greenhouse gas concentration in concert with the millenial-scale Dansgaard–Oeschger (D–O) climatic variability have been identified in Greenland and Antarctic ice cores (Petit et al., 1999; Flückiger et al., 2004). However, the influence of fire regime (fire intensity, severity, size, frequency at regional and centuries time-scale following Hu et al., 2006) on these variations is poorly understood due to the lack of high-resolution fire regime records covering this period. A recent synthesis of charcoal records covering the last 21 ka (Power et al., 2007) shows that spatial fire regime variations were not constant through this time related to changes of climate and local fuel load. High resolution deep-sea microcharcoal records covering the last glacial period (LGP) can provide new perspectives for understanding mechanisms of fire regime variability such as vegetation type, amount of fuel, climate changes through periods of drought, lightning storm position, human activity or orbital forcing.

The impact of D–O climatic variability on fire regime was detected for the first time in southwestern Iberia (Daniau et al., 2007), a region that experiences at present a frequent fire activity. The Iberian fire regime variability has been related to changes of fuel amount through shifts in vegetation between Greenland stadials (GS) including Heinrich events (HE), which experienced low fire regime associated with semi-desert vegetation, and Greenland interstadials (GI), which experienced high fire regime associated with open Mediterranean forest and heathland development. Changes in moisture and temperature conditions determine the type of vegetation, which in turn controls the amount of fuel and the fire return interval.

Fire regime and vegetation shift registered in southwestern Iberia between GS and GI have been related to prevailing atmospheric situations similar to the present-day positive and negative North Atlantic Oscillation (NAO) index, respectively (Daniau et al., 2007). The NAO is one of the major mechanisms responsible for the present-day wintertime temperature and precipitation patterns across the North Atlantic region. During the positive phase of NAO, the Mediterranean region experiences major drought because of the shift of the westerlies northwards, whereas a negative phase brings humidity to this region due to the weakening and southward displacement of westerlies to mid-latitudes. Winter moisture variation in southwestern France is, as in Iberia, negatively correlated to the NAO (Trigo et al., 2002). While a NAO-like pattern has been proposed to explain fuel availability and therefore fire regime during GS and GI in southwestern Iberia, we still do not know whether this atmospheric mechanism was at hand in regions located farther north.

This work has two main objectives: a) to document for the first time the fire regime of western France during the LGP, and b) to

* Corresponding author. Université de Bordeaux1, CNRS UMR5199 PACEA, Institut de Préhistoire et Géologie du Quaternaire, bât B18, Avenue des Facultés, 33405 TALENCE Cedex, France. Fax: +33 5 40 00 84 51.
*E-mail addresses:* al.daniau@ipgq.u-bordeaux1.fr (A.-L. Daniau), mf.sanchezgoni@epoc.u-bordeaux1.fr (M.F.S. Goñi), jm.duprat@orange.fr (J. Duprat).

0033-5894/$ – see front matter © 2009 University of Washington. All rights reserved.
doi:10.1016/j.yqres.2009.01.007

examine whether the fuel amount is, as in southwestern Iberia, the main factor controlling the millennial-scale fire regime variability in this region. For this, we analysed microcharcoal particles preserved in deep-sea core MD04-2845 in the Bay of Biscay at the latitude of Bordeaux. Complementary analysis of organic carbon on this core has been carried out in order to understand better the microcharcoal signal. Preliminary $\delta^{8}O$ isotopic measurements and previous studies of this core (carbonates, ice-rafted debris, planktonic foraminifera, pollen) have shown that it covers Marine Isotope Stage (MIS) 7 to 1 and revealed the impact of D–O climatic variability and Heinrich events in the ocean and on land (Sánchez Goñi et al., 2008). The direct correlation between past fire regime and these climatic proxies, in particular vegetation shifts, allows the discussion of the complex relationships between fire and climate.

## Environmental setting

### *Present-day vegetation, fire and climate*

Western France extends from 42°N to 48°N (Fig. 1) and comprises essentially the Loire–Britany and the Adour–Garonne river basins. This region is characterised by a temperate and oceanic climate. Winter precipitation in its southern part is particularly influenced by the NAO (Trigo et al., 2002; Dupuis et al., 2006). Annual precipitation of the Loire–Britany basin is 500–700 mm and 600–1000 mm for the Adour–Garonne basin. The specific region covered by mountains (the Massif Central and the Pyrenean) receive more than 1500 mm. The mean temperatures in winter vary from 0 to more than 8°C on the Atlantic coast, and from 15 to more than 22°C in summer (Serryn, 1994). The region is colonised today by Atlantic vegetation (Fig. 1) characterised by deciduous forests (mainly oaks, ash, beech, birch) and coniferous trees restricted to montane and some southern maritime areas, and by semi-natural grasslands (Polunin and Walters, 1985).

Compared to Spain, Portugal, Italy and Greece, France does not experience a high fire activity. The average of 30,738 ha of burnt wooded area and 5218 forest fires for the period AD 1980–2000 represent only 4% and 10%, respectively, of that of the other countries (European Commission, 2001). Fire activity in France is mainly concentrated in its Mediterranean part, during summer months (July and August). The western part of France is, on the whole, not affected by large fires, but local fires caused by lightning do occur (http://www.feudeforet.org/). However, as the present-day incidence and spatial distribution of fires resulting from lighting strikes is restricted by human activities, this type of ignition may have been more important in the past.

### *Oceanic surface circulation and wind patterns*

The current circulation pattern in the Bay of Biscay (Fig. 2) is characterised by a mean southward surface circulation during summer, the formation of eddies near the shelf break and a weak flow of the slope current. During winter, the mean surface circulation is dominated by a strong poleward intrusion of the slope current along the Iberian Peninsula and the Armorican and Celtic slopes, with a branch of westward orientation inside the Bay of Biscay, generating a particular cyclonic cell circulation centred at 46°N, 6.5°W (Durrieu de Madron et al., 1999; Colas, 2003). This poleward slope current (the Navidad current) in the winter season brings warm surface water into the Bay of Biscay and may affect biological productivity (Garcia-Soto et al., 2002). Its strength depends on the wind pattern over the Bay

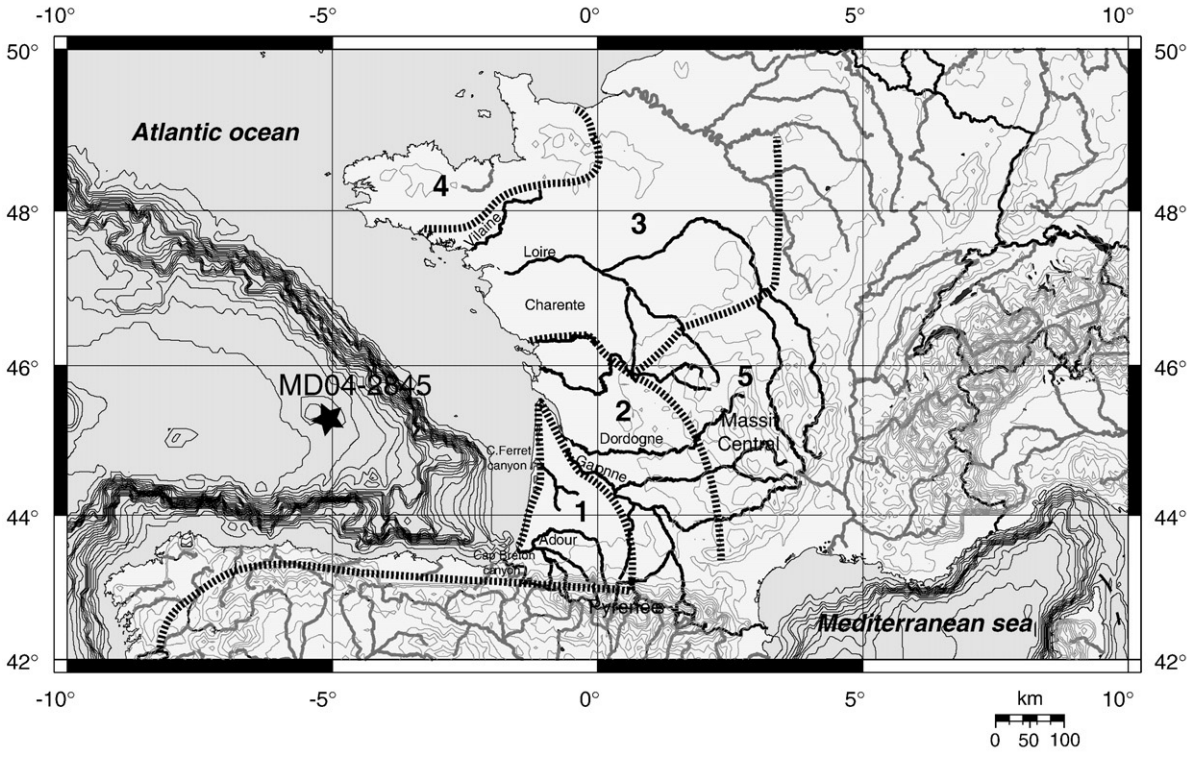


**Figure 1.** Map of France showing the location of core MD04-2845 (filled star). Black dotted lines represent the division of the Atlantic and Sub-Atlantic vegetation domains simplified from Ozenda (1982). Area 1: Southwestern France is characterised by vegetation composed of *Quercus robur*, *Q. pyrenaica*, *Castanea sativa*, *Pinus pinaster* with some *Q. suber*. Area 2: This region presents a mosaic of *Quercus pubescens*, *Q. robur* and *Q. petrae*. Some *Q. ilex* is found near the coast. Area 3: Vegetation of the central-western part of France is mainly characterised by a mosaic of *Q. robur* on alluvial soils and *Q. petraea* associated with hornbeam (*Carpinus betulus*) on slope and drained areas. Area 4: Vegetation of the north-western part, characterised by a high level of precipitation, is a mosaic of three main floristic associations including *Fagus* forest, *Fagus-Quercus* robur forest and heathland community dominated by *Calluna* and *Ulex*. Near the coast, *Fagus* forest is replaced by *Quercus-Fraxinus* forest. Area 5: The Massif Central is colonised mainly by *Q. robur*, *Q. petraea*, *Q. pubescens* and *Castanea sativa* between 600 and 800 m. *Fagus*, *Fagus-Pinus* forest, heathland, *Ulex*, and *Pinus sylvestris* forest are found above. Between 1500 and 1600 m the vegetation is composed of heathland of *Calluna* and *Juniperus sibirica*.

https://doi.org/10.1016/j.yqres.2009.01.007 Published online by Cambridge University Press

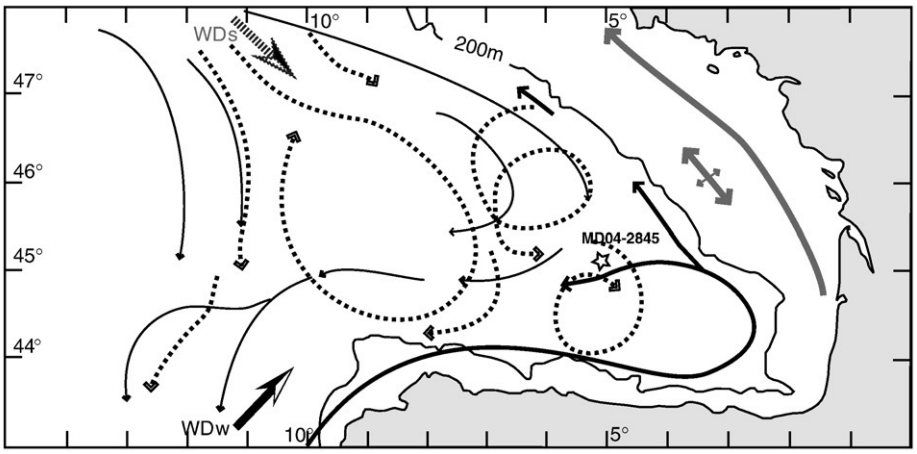


**Figure 2.** Map of oceanic circulation and wind directions in the Bay of Biscay during summer and winter situations (modified from Durrieu de Madron et al., 1999 and Koutsikopoulos and Le Cann, 1996). Below 200 m depth, oceanic circulation during winter is represented by black lines (with a strong poleward of the slope current corresponding to the Navidad current). Black dotted lines represent oceanic circulation during summer. Shelf residual current (along the coast) and wind-induced currents (grey double arrows) are found on the shelf. Arrows represent dominant wind directions. WDw (black arrow): wind direction in winter. WDs (grey dotted arrow): wind direction in summer.

related to the NAO, with a low NAO index leading to an intensified Navidad current (Garcia-Soto et al., 2002).

The mean wind direction over the Bay (Fig. 1) is from northwest in summer and from southwest in the winter season. However, a southward direction towards northern Iberia prevailed inside the bay for both situations (Colas, 2003). Upwellings appear during spring and summer period along the shelf area in relation to wind blowing to the coast (Heaps, 1980). Northwesterly to northerly wind events create coastal upwellings off southern Brittany, Vendée and Landes. Westerly winds generate upwelling to the north of the Loire (Froidefond et al., 1996; Lazure and Jégou, 1998; Puillat et al., 2004). Core MD04-2845 is outside of these upwelling areas.

*Morphology and recent sedimentation*

The Bay of Biscay is characterised by a continental shelf oriented NW–SE along the French coast and E–W along the Spanish coast, with a platform relatively flat. Its large width along the French coast prevents direct feeding on the shelf break by bottom nepheloid layers (Jouanneau et al., 1999) except for the region of the Cap-Ferret Canyon (Ruch et al., 1993). Two sedimentary systems characterise the continental shelf of this bay, an inner shelf (<100–120 m) and an outer shelf (>120 m) showing a general grain-size fining southward (Allen and Castaing, 1977). Pre- and early Holocene offshore mud and sands occupy the zone between 75 and 120 m depth, and coarse sands and gravels carried by rivers between 30–75 m, probably related to the influence of the Gironde paleoriver detected 50 km seaward of the estuary mouth (Lericolais et al., 2001).

Rivers (Fig. 1) are the main sources of fine sediments (including microcharcoal and pollen) to the Bay of Biscay, taking into account that westerlies are the dominant winds in the Bay. The main rivers, the Garonne and the Dordogne feeding the Gironde estuary, the Loire, the Vilaine, the Charente and the Adour rivers, deliver about $2.5\times10^6$ t $yr^{-1}$ of continental fine sediments, with the Gironde estuary accounting for 60% of this amount (Jouanneau et al., 1999). The continental suspended matter which spreads out from the Gironde estuary on the shelf is transported to the north along the coast by a surface turbid plume (Castaing, 1981) and may be carried to the Cap-Ferret Canyon in a bottom nepheloid layer (Ruch et al., 1993). However, an estimated $0.9\times10^6$ t $yr^{-1}$ of fine sediments could reach the slope and eventually the open ocean (Jouanneau et al., 1999).

Experimental studies on the present-day pollen–vegetation relationship confirms that marine pollen assemblages from the southwestern French margin represent an integrated image of the regional vegetation, including coastal, low and high altitude areas (Turon, 1984). Pollen assemblages preserved in core MD04-2845 therefore reflect the vegetation colonising both hydrographic basins with headwaters located in the Massif Central and the Pyrenees, respectively.

## Materials and methods

*Core location, sampling and chronostratigraphy*

Deep-sea core MD04-2845 (45°21′N, 5°13′W; 4175 m water depth) (Fig. 1) was collected during the Alienor cruise in 2004 in the Bay of Biscay using the CALYPSO Kullenberg corer aboard the Marion Dufresne vessel. The site is located 350 km from the nearest coastline on the Gascogne Seamount, without influence of turbidite currents. The sediments are mainly composed of clayey mud with sparse silty laminations, with 10–65% carbonate. Observations of X-ray analysis using SCOPIX image-processing have shown a well preserved sedimentary sequence not perturbed by turbidites in the analysed part of core MD04-2845 between 760 and 2245 cm depth. A sedimentary hiatus appears between 1714 and 1740 cm depths.

Carbonate content measurements and onboard sediment reflectivity curve along with IRD counting, polar foraminifer *Neogloboquadrina pachyderma (s)* percentages and foraminifer assemblage-derived sea surface temperatures (SST) of core MD04-2845 define the last interglacial, D–O events and Heinrich events. To compare fire regime of western France with that recorded in southwestern Iberia (Daniau et al., 2007), the age model of the marine core MD04-2845 is based on that of the southern Iberian margin core MD95-2042 (37°14′N, 10°11′W), which is AMS $^{14}$C dated and calibrated to GISP2 and GRIPSS09sea chronologies, assuming that changes in the polar front position were synchronous in the North Atlantic region (Shackleton et al., 2000, 2004; Bard et al., 2004). Control points used for the glacial interval of core MD04-2845 are derived from the correlation of the onset of GI and boundaries of HE detected in this core with those identified in core MD95-2042 (see synthetised table in Sánchez Goñi et al., 2008).

For the interval 680–892 cm (Table 1), we add 4 control points derived from the age model of the Iberian core used in Daniau et al. (2007). Ages of these control points are in good agreement with linear age model obtained from 10 AMS $^{14}$C ages obtained for core MD04-

https://doi.org/10.1016/j.yqres.2009.01.007 Published online by Cambridge University Press

**Table 1**
Chronostratigraphic model for core MD04-2845.

| Lab code/*event* | Core depth (m) | Material | Conv. AMS $^{14}$C age kyr (−400 yr) | Error yr± | 95.4% (2$\sigma$) Cal BP age ranges | (1) Cal BP age (ka) median probability | (2) Bard et al. (2004) age (ka) | (3) Control points (ka) based on MD95-2042 chronology |
|---|---|---|---|---|---|---|---|---|
| SacA-002960 | 5.2 | *G. bulloides* | 16.890 | 150 | 19.782:20.365 | 20.03 | | |
| *HE2/GIS2* | *6.8* | | | | | | | *23.95* |
| SacA-002961 | 6.9 | *N. pachyderma (s)* | 20.420 | 140 | 24.016:24.890 | 24.44 | | |
| SacA-002962 | 7.1 | *N. pachyderma (s)* | 20.710 | 140 | 24.426:25.405 | 24.88 | | |
| SacA-002963 | 7.7 | *N. pachyderma (s)* | 21.860 | 160 | | | 25.82 | |
| SacA-002964 | 7.9 | *N. pachyderma (s)* | 22.150 | 170 | | | 26.14 | |
| *Base HE2* | *8.1* | | | | | | | *26.25* |
| SacA-002965 | 8.5 | *G. bulloides* | 24.050 | 210 | | | 28.22 | |
| *Onset GIS3* | *8.5* | | | | | | | *27.84* |
| SacA-002966 | 8.6[a] | *N. pachyderma (s)* | 24.680[a] | 230 | | | 28.89[a] | |
| SacA-002967 | 8.7[a] | *N. pachyderma (s)* | 24.630[a] | 230 | | | 28.84[a] | |
| SacA-002968 | 8.9[a] | *G. bulloides* | 25.230[a] | 240 | | | 29.48[a] | |
| *HE3/GIS4* | *8.92* | | | | | | | *29.00* |
| SacA-002969 | 9.0[a] | *N. pachyderma (s)* | 24.870[a] | 240 | | | 29.10[a] | |

A mean age (ka) has been calculated for consecutive levels (8.6–8.7 and 8.9–9 m) before applying linear interpolation to estimate age difference between control points (3) and ages based on calibrated AMS $^{14}$C (1,2).
[a] Levels presenting small AMS $^{14}$C inversions.

2845 in the interval HE3/GI4 to HE2/GI2 (mean age difference <400 yr). The samples presenting conventional AMS $^{14}$C younger than 21,786 $^{14}$C yr BP were calibrated by using CALIB Rev 5.0 program and "global" marine calibration data set (marine 04.14c) (Stuiver and Reimer, 1993; Hughen et al., 2004; Stuiver et al., 2005). $^{14}$C radiometric ages older than 21,786 $^{14}$C yr BP were calibrated by matching the obtained conventional AMS $^{14}$C with the calendar ages estimated for MD95-2042 deep-sea core by Bard et al. (2004).

The core was sampled every 5 cm between 2245 cm and 760 cm for microcharcoal and organic carbon content analyses; this interval encompasses the end of MIS 6 to MIS 2.

### *Image analysis for microcharcoal counting*

A total of 294 samples were analysed for microcharcoal using automated image analysis in transmitted light. Microcharcoal preparation technique followed the work of Daniau et al. (2007). Chemical treatment was performed over 24 h on 0.2 g of dried sediment and involved the addition of 5 mL of 37% HCl; 5 mL of 68% $HNO_3$; 10 mL of 33% $H_2O_2$. This chemical treatment is used to remove pyrites, humic material, labil or less refractory organic matter (OM) and to bleach non-oxidised OM. Dilution of 0.1 was then applied to this residue and this suspension was filtered onto a cellulose acetate membrane containing nitrocellulose of 0.45 µm porosity and 47 mm in diameter. A portion of the membrane was dissolved onto a plexiglass slide with ethyl acetate before gentle polishing with alumin powder of 200 Å. The use of polish slide (used classically in petrographic analysis) for image analysis is better than the previously assembling technique consisting of mounting the portion of the membrane onto a slide with Canadian balsam (Daniau et al., 2007) as the focus on the edge of microcharcoal is improved. The slides were scanned with an automated Leica DM6000M microscope at ×500 magnification. In order to have a good statistical representation of each sample, 200 view-fields (200 images) of 0.0614 mm$^2$ were "grabbed" in color with a 1044×772 pixels digitising camera (1 pixel = 0.276 µm). The surface scanned by the microscope represents a surface area of 12.279 mm$^2$.

Microcharcoal recognition was performed by using a program of image analysis developed in this study with LeicaQwin software. The subroutine written for microcharcoal identification during image analysis procedure was established by a simultaneous visual identification of microcharcoal in transmitted light following criteria from Boulter (1994), namely black debris, opaque, with sharp edges (see also Enache and Cumming, 2006) and petrographic criteria in reflected light, that is with visible plant structures characterised by thin cell walls and empty cellular cavities, or particles without plant structure but of similar reflectance than that of previous ones (Noël, 2001). In a controlled light adjustment, a threshold value in red, green, blue (RGB) color was defined to identify microcharcoal based on several observations of particle on different slides.

From measured variables of microcharcoal (surface area, length, width, elongation, number) we calculated for each sample:

a) the concentration of microcharcoal (CCnb): number of microcharcoal per gram (nb g$^{-1}$)
b) the concentration of microcharcoal surface (CCsurf), which is the sum of all surfaces of microcharcoal in one sample per gram (µm$^2$ g$^{-1}$). This is to avoid the overrepresentation of microcharcoal concentration as the result of potential fragmentation during production (Théry-Parisot, 1998) or transport.

The three-point running mean "MCCnb" and "MCCsurf" was also calculated for CCnb and CCsurf, respectively, to be able to compare fire regime with vegetation history of the same core (resolution of 10 cm). The term MCC will be used as global mean average microcharcoal concentration representing microcharcoal concentration variation of number or surface of microcharcoal (as the two microcharcoal concentrations covary, see below).

Replicate analysis was done on 10 samples randomly selected from core MD04-2845, analysed ten times each. Experimental standard deviations were calculated with the equation below. The confidence interval at 95% (see curve in Fig. 3) is derived from the Student's $t$-distribution for $n-1$ degrees of freedom ($x_i \pm t^*s$ with $t = 2.262$).

$$s = \sqrt{\frac{1}{n-1}\sum_{i=1}^{n}(x_i - \overline{x})^2}$$

The minimum of variation of MCC discussed below is higher than the widen confidence interval so that variations observed in MCC curve are not related to an artefact of sampling bias.

### *Particulate organic carbon (POC) analysis*

The organic carbon (OC) content was determined directly on dry weight material sediment by combustion in an LECO CS 200 analyzer (Etcheber et al., 1999) on the same sample depth as that used for microcharcoal analysis. Around 50 mg of powdered and homogenized samples were acidified in crucibles with 2 N HCl to destroy carbonates and then dried at 60°C to remove inorganic carbon and most of the remaining acid and water. The OC analysis was performed by direct combustion in an induction furnace, and the

https://doi.org/10.1016/j.yqres.2009.01.007 Published online by Cambridge University Press

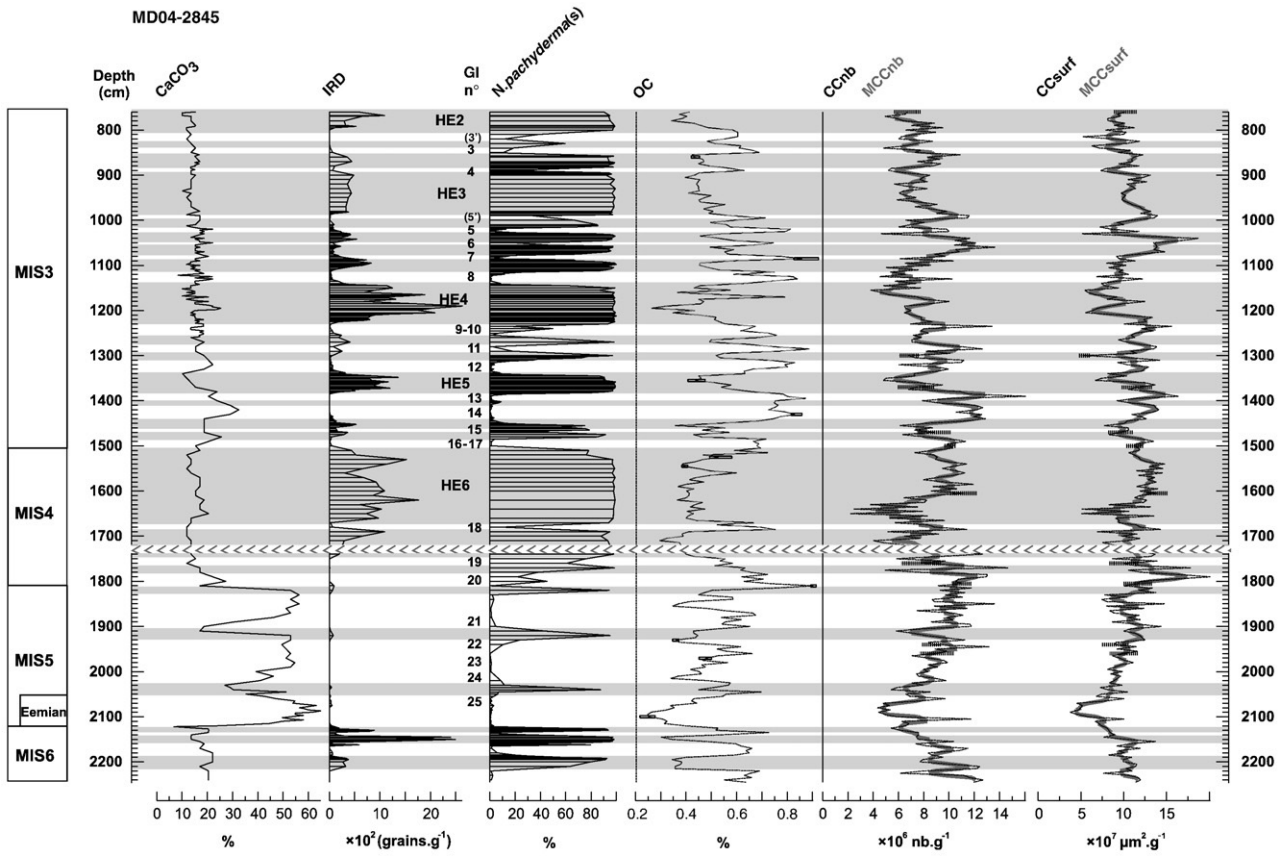


**Figure 3.** Results from microcharcoal and organic carbon content and comparison with other marine proxies of core MD04-2845. All records are plotted versus depth. Limits of Marine Isotopic Stages (MIS) and the Eemian Interglacial are also indicated. From left to right: (a) the carbonate percentages ($CaCO_3$), (b) the ice rafted debris (IRD) concentration, (c) the polar foraminifera *Neogloboquadrina pachyderma* (s) abundance percentages, (d) the organic carbon content (OC) percentage, (e) the microcharcoal number concentration curve (CCnb) and the three-point running mean (MCCnb), (f) the microcharcoal surface area concentration (CCsurf) and the three-point running mean (MCCsurf). Grey rectangle shown on the OC curve represents the greatest lower and least upper bound of replicates. Dotted bar on microcharcoal concentration curve (CCnb and CCsurf) indicate the 95% confidence interval. Grey bands indicate Heinrich events and other Dansgaard–Oeschger stadials. Heinrich events are identified on the basis of peaks in ice rafted debris (IRD), high polar foraminifera (*N. pachyderma* s.) percentages and AMS $^{14}C$ ages. Greenland interstadial numbers (GI) are also shown. 1714–1740 cm: sedimentary hiatus.

$CO_2$ formed was determined quantitatively by infrared absorption. Replicate analyses were performed on 10 selected samples reanalysed 6 times each (greatest lower and least upper bound are indicated in Fig. 3).

## Results

### *Microcharcoal analysis*

Concentration of CCnb varies between $218.4\times10^4$ and $1607\times10^4$ nb $g^{-1}$ (Fig. 3). Concentration of CCsurf varies between $3731\times10^4$ and $20{,}137\times10^4$ µm$^2$ $g^{-1}$. CCnb and CCsurf are positively correlated ($r=0.75$; $R^2=0.56$). Visual inspection of MCCnb and MCCsurf reveals high variability superimposed to a long-term trend. A long-term decreasing trend characterises the end of MIS 6 until the middle part of the Eemian, the MIS 4 until the beginning of HE6, and the intervals between GI14–HE4 and GI6–HE2. A long-term trend of increasing values of MCC occurs from the end of the Eemian to the onset of MIS 4.

The high variability of MCCnb and MCCsurf superimposed to the long-term trend shows low values or decreasing values during stadials of MIS 5 and 6 (except GS20), and during GS and HE except for the middle part of HE6 and 4, GS8, GS7, GS4 and GS3. Each of HE are characterised by three phases: a phase of relatively high MCC bracketed by two phases of low MCC. A pronounced decrease of MCC occurs at the end of HE4 and HE3, while HE6 presents a rather different pattern with a strong decrease of MCC at the beginning of the event.

### *Organic carbon (OC)*

The OC of core MD04-2845 (Fig. 3) varies between 0.248 and 0.903% (average value of 0.53%) which is comparable to the OC reported in the Bay of Biscay for sediments from the shelf (<0.5%) or deep ocean (average value: 0.5–1%) (Etcheber et al., 1999). The OC values are comparable between the last interglacial (average value of 0.49%) and the LGP (average value of 0.55%). The OC is highly variable for the LGP and parallels the D–O climatic variability with high values during GI and low values during GS and HE. During the last interglacial period, three gradual increases of OC occurred during the Eemian—GS25, GI23–22, GI21 and GI20. The end of MIS 6 presents the same pattern than the LGP with peaks of OC corresponding to interstadials and low values of OC during stadials.

### *Time-series analysis*

To extract the significant periodicities of our proxies, spectral analysis was applied on linear detrended OC content and microcharcoal concentration (CCsurf and CCnb) before applying the Lomb periodogram algorithm (Past software). Periodicities have been selected for a 0.01 (99%) significance level. Several millenial periodicities are detected in the proxies (see Fig. 4). Most notably,

https://doi.org/10.1016/j.yqres.2009.01.007 Published online by Cambridge University Press

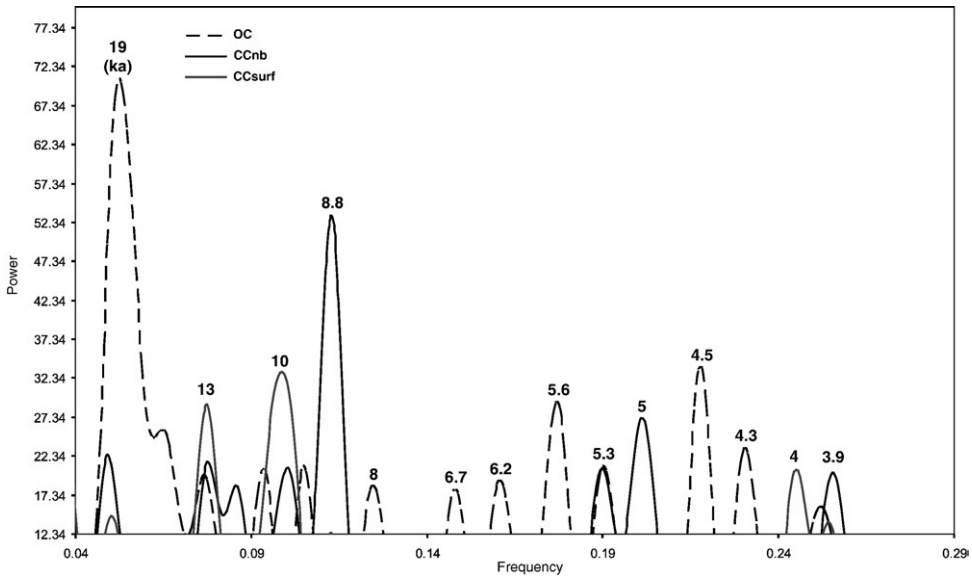


**Figure 4.** Spectral analysis applied to linear detrended OC content and microcharcoal concentration (CCsurf and CCnb) before applying the Lomb periodogram algorithm (Past software). Periodicities (ka) have been selected for a 0.01 (99%) significance level. Peaks in the spectrum are presented with frequency (*X*-axis) and power value (*Y*-axis) (units proportional to the square of the amplitudes of the sinusoids present in the data).

periods close to the precession (19–20 ka) are detected for OC and microcharcoal concentration. CC presents well-marked periods of 13, 10 and 8.8 ka.

## Discussion

### *Last glacial oceanic circulation and wind direction changes: implications for microcharcoal signal interpretation*

In order to test whether millenial-scale MCC variation is related to actual changes in fire regime and to verify that MCC variation is independent of changes in aeolian or fluvial sedimentary input, we have used other climatic proxies (pollen, foraminifera derived-SST, OC and $CaCO_3$). OC content parallels the D–O climatic variability with an alternation of high and low OC values during GI and GS, respectively (Fig. 3). OC content in marine cores is derived from marine productivity, although a fraction of continental material may affect it (Pailler and Bard, 2002). The absence of correlation over the record of core MD04-2845 between OC and terrestrial material such as microcharcoal and pollen ($r=0.34$, $p<0.01$ for OC content and microcharcoal concentration, $r=0.16$, $p<0.1$ for OC and pollen concentration) implies that such OC variations cannot be explained only by changes of continental organic matter supply via wind or rivers. Additionally, $CaCO_3$ being free of dissolution because of the core location above the carbonate compensation depth (Kennett, 1982), no significant correlation between OC and $CaCO_3$ contents ($r=-0.13$, $p<0.02$) indicates that the OC might derive from non-calcifying species such as diatoms or silicoflagellates. Coccoliths such as *Emiliana huxelyi*, *Gephyrocapsa* and *Coccolithus pelagicus*, which are currently associated with an increase of diatoms and silicoflagellates in this region (Beaufort and Heussner, 1999), were indeed observed during interstadials in our core (e.g., GI 17–16, J. Giraudeau, pers. comm.). This suggests that an increase of OC during GI reflects an increase of marine productivity. The OC pattern in core MD04-2845 is similar to the pattern of dinoflagellates productivity in the marine core MD03-2692 located on the Celtic margin during MIS 6, where higher concentrations during interstadials and lower ones during stadials are observed (Penaud, unpublished data). We therefore consider OC to be essentially a proxy of marine productivity in core MD04-2845.

Last glacial productivity changes revealed by a core located off Lisboa were related to variations in Portugal's upwelling system (Pailler and Bard, 2002). However, the Gascogne seamount is far from regions affected today by upwellings in the Bay of Biscay, namely the shelf break or river plumes. This site was also outside the direct influence of upwelling during the LGP because the shelf break was still drowned at the maximum lowstand sea level (maximum of −120 m depth for the last glacial maximum). Therefore, a different mechanism to that explaining the OC content variation in the Iberian margin must be responsible for the observed shifts in OC between GS and GI in our core.

Forest development detected in core MD04-2845 during GI (Fig. 5) suggests an increase of temperatures and precipitation. At present, the increase of humidity as well as river run-off in southwestern France is related with the negative mode of the NAO (Trigo et al., 2002; Dupuis et al., 2006). Climatic conditions in this region during GI might be related, as suggested for southern Iberia (Combourieu Nebout et al., 2002; Moreno et al., 2002; Sánchez Goñi et al., 2002), to a prevailing negative NAO-like situation. Under this climatic regime, SST warming might also be linked to enhanced influence of a warm paleo Navidad current, as occurs today during negative NAO index (Garcia-Soto et al., 2002), favouring productivity blooms and OC increase during the GI. Moreover, our hypothesis of the paleo-Navidad current strengthening under a negative NAO-like mode during GI is consistent with the observed weakening of Mediterranean Outflow Water (MOW) at that time (Voelker et al., 2006; Toucanne et al., 2007). The formation of western Mediterranean Deep Water, which likely was a major source of the MOW during the last glacial (Myers et al., 1998; Voelker et al., 2006), is at present positively correlated to the NAO (Rixen et al., 2005).

The comparison between this past oceanic scenario pattern with the modern oceanic and atmospheric circulations (Fig. 2) suggests that GI would be, as in the modern situation, more influenced by southwesterly winds (winter situation) than GS periods that were characterised by prevailing northwesterlies (summer situation). As both wind systems come from the ocean, we do not expect therefore a substantial aeolian contribution of microcharcoal to the Gascogne

https://doi.org/10.1016/j.yqres.2009.01.007 Published online by Cambridge University Press

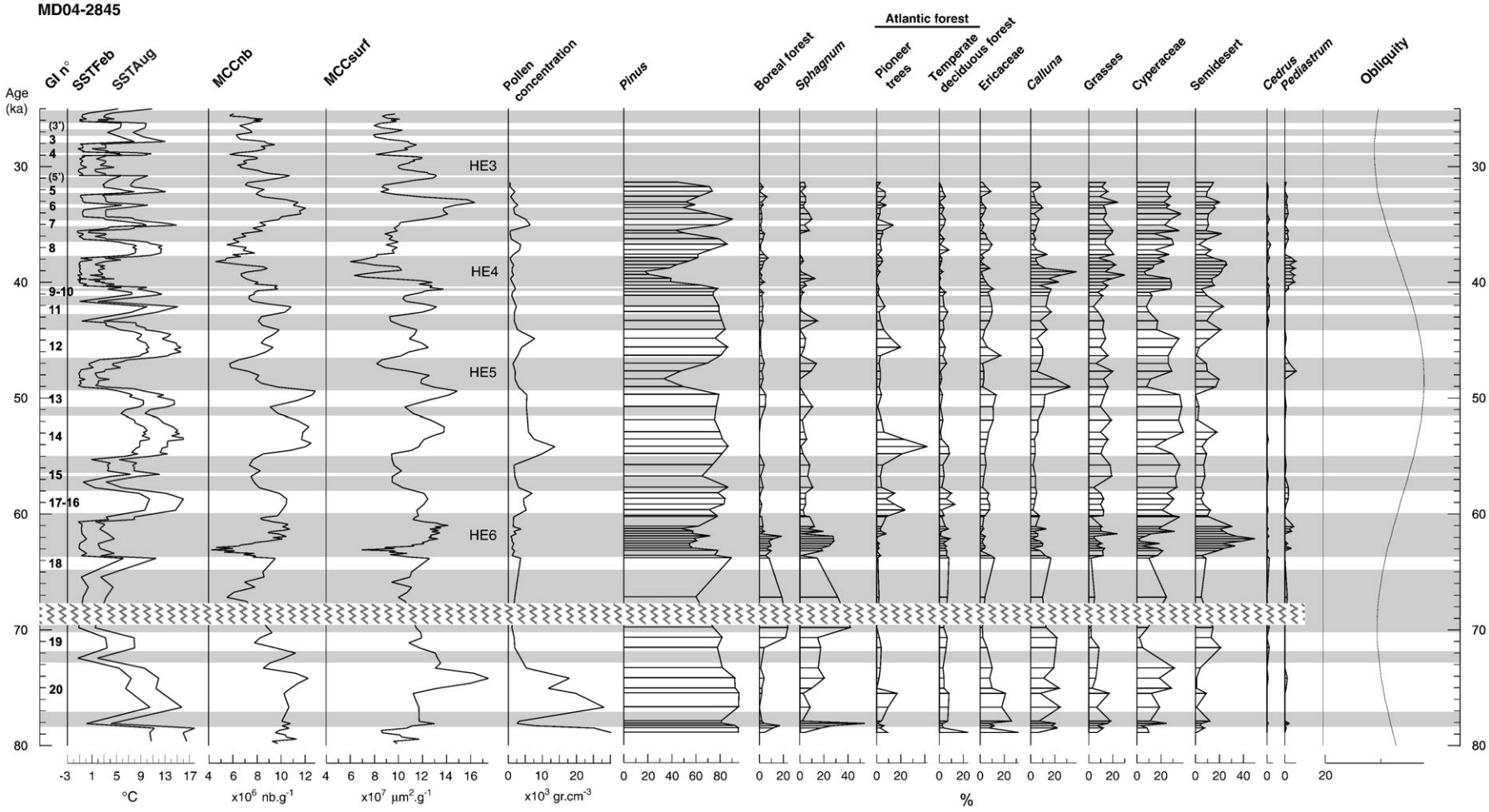


**Figure 5.** Comparison between microcharcoal trends and climatic proxies from core MD04-2845. All records are plotted versus age. From left to right: (a) sea surface temperature derived from foraminifera assemblages for February (SSTFeb) and August (SSTAug), (b) three-point running mean microcharcoal number concentration curve (MCCnb), (c) three point-running mean microcharcoal surface area concentration curve (MCCsurf), (d) pollen concentration, (e) to (p) pollen group percentage curves, (q) obliquity curve from Laskar et al. (2004). Boreal forest: at 90% *Picea*, *Alnus* and *Salix*; pioneer trees: mainly *Betula*, Cupressaceae and *Hippophäe*; temperate deciduous forest: deciduous *Quercus*, *Carpinus* and *Corylus*; grasses: *Poaceae*; semi-desert: Chenopodiaceae, *Ephedra* and *Artemisia*. Although *Betula* can also belong to boreal forest, percentage variation in our record does not follow the *Picea* pattern, which suggests its inclusion in the Atlantic forest. 68–70 ka: sedimentary hiatus.

seamount during the different phases of the LGP. This is also supported by the sporadic presence of the North African wind-pollinated *Cedrus* tree pollen in the record (Fig. 5), which suggests negligible input of charcoal coming from the south. As with other regions in western Europe (Van Huissteden et al., 2001), the Bay of Biscay was likely characterised by prevailing westerlies during the LGP, suggesting that MCC variability is not controlled by changes in wind directions.

MCC variation in core MD04-2845, retrieved at 350 km from the coast and on a seamount, would be only affected by dilution related to the biogenic or terrigenous hemipelagic input or changes in fluvial sedimentary transfer. The lack of correlation between non-carbonate sedimentary fraction (1-$CaCO_3$) or carbonates and microcharcoal concentration ($r = \pm 0.408$ with CCnb, or $r = \pm 0.21$ with CCsurf ($p < 0.01$)) for the LGP suggests that neither biogenic nor terrigenous material dilute microcharcoal concentration and that MCC variation is not related to changes in fluvial discharges.

MCC variation is therefore not related to changes in aeolian or fluvial sedimentary input, implying that changes in MCC represent variation in regional microcharcoal production and, therefore, in fire regime of western France. Intervals of high MCC values identify periods of strong fire regime, while those marked by low values reveal weak fire regime phases.

### *Fire regime, vegetation composition and climate in western France during the last glacial period*

Fire regime is highly variable all along the record, especially during the LGP (Fig. 5): low fire regimes are detected during GS and HE and high fire regimes during GI. This strong fire regime variability may reflect climatic changes, namely succession of dry and humid periods, involving shifts in lightning storm position, changes in fire-sensitive species or variations in fuel availability. In addition, variations of fire regime have likely an impact on vegetation succession. In order to discuss short and long-term fire–climate–vegetation relationship, we have compared fire regime changes and fluctuations in vegetation cover and composition (Fig. 5). The vegetation of core MD04-2845 shows that *Betula-Pinus*-deciduous *Quercus* forest expanded during GI and steppic plants (*Artemisia*, Poaceae, heaths and sedges) dominated during the cold and dry GS (Sánchez Goñi et al., 2008).

No continuous and well-dated pollen terrestrial records identifying the millennial-scale variability are available in western France. Only the multiproxy study of the Cestas soil, located in southwestern France and reliably related with HE2 (Bertran et al., 2008), sheds light on local vegetation environments at low altitudes. These environments are similar to those described from marine pollen record MD04-2845 and mainly composed by steppic plants such as Poaceae, *Helianthemum* and *Artemisia*, sedges associated with local shrub dominated by Myrica and Ericaceae.

#### *Dansgaard–Oeschger interstadials and stadials*

Major differences in fire regime in western France between GS (low fire regime) and GI (high fire regime) are not associated with a particular taxon. Increase in fire regime is associated with periods of afforestation corresponding to the establishment of *Betula-Pinus-deciduous Quercus* open forest during GI, and low fire regime with steppic plants during GS. Some increase of fire regime are also associated to certain peaks of Ericaceae and *Calluna* on which repeated fires encourage their regeneration (Bradshaw et al., 1997; Mouillot et al., 2002; Calvo et al., 2002). Beyond the influence of the type and density of the vegetation on the fire regime through changes in fire frequency or severity, increase of microcharcoal concentration during periods of afforestation suggests the increase of microcharcoal production related to increase of woody fuel and biomass accumulation during GI as total plant biomass in forested areas is generally higher than open ground formations (Magri, 1994). This increase of woody fuel during GI indicates an increase of humidity and associated sea and air surface temperature warming as likely the result of a prevailing negative NAO-like index.

Increase of fire regime related to woody fuel availability for the LGP has been already suggested by Daniau et al. (2007) for southwestern Iberia and inferred from the strong correlation between MCC and forest percentage curves. This hypothesis is supported by the simulation of Ni et al. (2006) for semi-arid regions where lack of fuel, related to drought, often limits the incidence of fire. Although the relationship between fire regime and fuel changes occurs also in western France during the LGP, the tight correlation found in Iberia is less evident in western France. This suggests that in addition to fuel, a direct climatic control may have operated on the fire regime variability of the latter region during the LGP. The reason may be that D–O climatic variability has a lesser impact on vegetation shift between GS and GI which allows the development of a mosaic of vegetation with a dominance of grasses through both GS and GI. At present, a sharp contrast of precipitable water exists in Iberia between negative NAO (high precipitation) and positive NAO (marked drought) situations. Although the same pattern occurs in southwestern France, the contrast of precipitable water is less marked in this region (Trigo et al., 2002). Sánchez Goñi et al. (2008) show that the boundary of the Mediterranean region was similar to that of the present day during GI. This would imply that a similar gradient of precipitable water than that observed at present between the two regions may occur during GI and suggests that during GS (positive NAO-like situation), moisture content in western France is sufficient to develop a continuous vegetation cover, mainly grasses, while lack of winter moisture in southwestern Iberia triggered the development of semi-desert vegetation.

#### *Zooming in on Heinrich events 6, 5 and 4*

The vegetation of HE 6, 5 and 4 (Fig. 6), mainly composed of *Pinus* woodlands, some *Picea* (well developed during HE6), *Sphagnum*, *Calluna*, and Cyperaceae species, is typical of present-day Boreal or central European vegetation, characterised by evergreen coniferous forest and mires which indicate high rainfall areas (Polunin and Walters, 1985). The relative high percentages of *Artemisia* during HE indicates this species occupies drier soils.

*Heinrich event 4.* Fire regime during HE4 presents a three-phase structure (Fig. 6a). Decrease of fire regime at the beginning of HE4, phase (a), is contemporaneous with a large reduction by ~50% of *Pinus* percentages contemporaneous with the succession of Cyperaceae, *Sphagnum* and *Calluna* progressively dominating the pollen assemblage. Succession of Cyperaceae and *Sphagnum* indicates progressive colonisation of water-filled depressions by fens (minerotrophic peatland) then by bogs (ombrotrophic), which is the typical ecological succession of peatland (mire) (McNamara et al., 1992). This plant succession suggests also a vegetation of transitional mire which forms a mosaic of bog and fen, or occurs where bog and fen succeed each other (Polunin and Walters, 1985). Whereas the development of *Sphagnum* indicates moist or waterlogged environments, this species colonises the upper part of the water table (Rochefort et al., 2002). Most *Sphagnum* species are absent or poorly represented in habitats with an extremely fluctuating water table compared to *Calluna vulgaris,* which prefers considerable fluctuations (Laitinen et al., 2007).

The progressive dominance of *Calluna* at the end of this phase and the disappearance of *Sphagnum* suggests an increase of the water table and surface runoff produced by higher precipitation. Even if summer convective rain would promote fire ignitions, relative strong moist conditions would have slowed down fire propagation, leading to the decrease of fire regime during the first phase of HE4, in particular in a low fuel availability environment. Increase of fire regime period, phase (b), starts with the beginning of *Pinus* forest development associated with the decline of *Calluna* and the weak

https://doi.org/10.1016/j.yqres.2009.01.007 Published online by Cambridge University Press

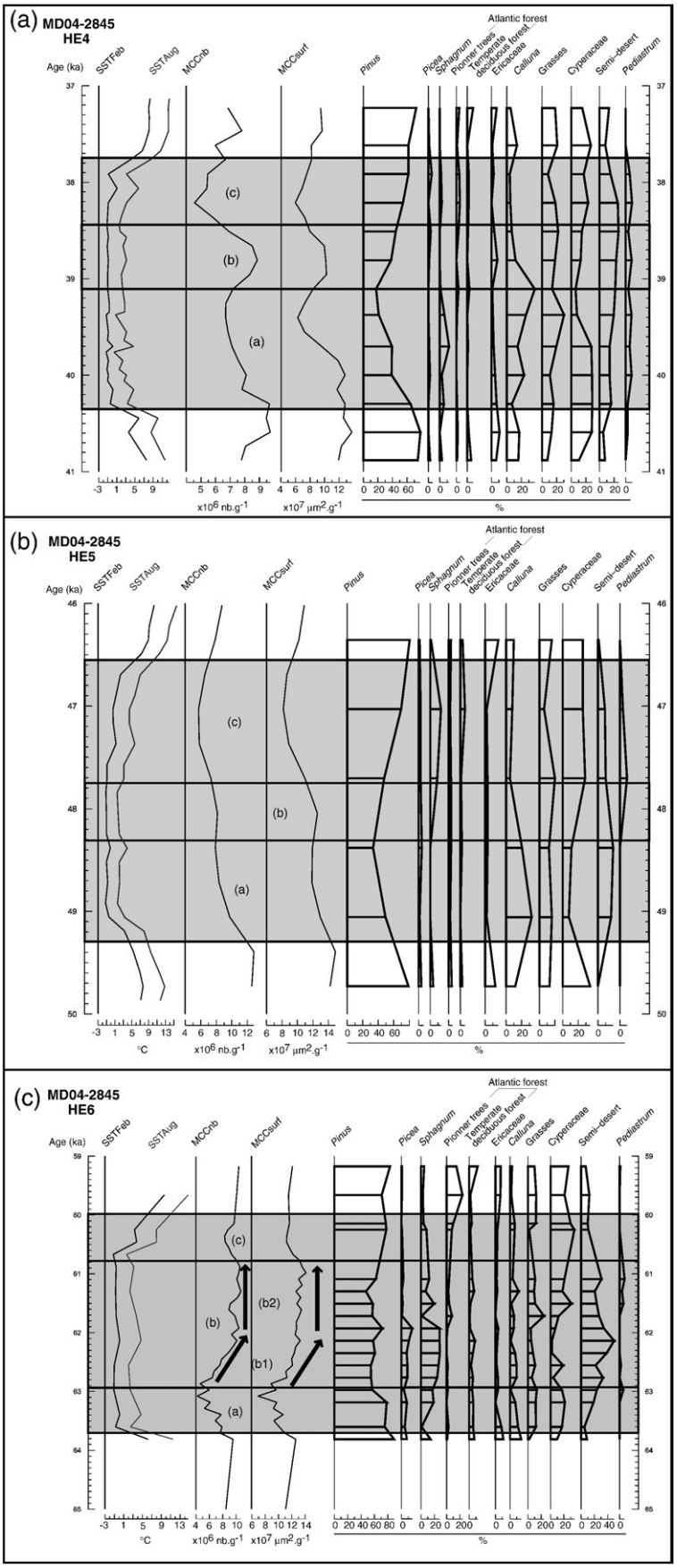


**Figure 6.** Comparison between microcharcoal concentration and climatic proxies during Heinrich events (HE). (a) HE4, (b) HE5, (c) HE6. All records are plotted versus age. (a) Sea surface temperature of February (SSTFeb) and August (SSTAug), (b) three-point running mean microcharcoal number concentration curve (MCCnb), (c) three point-running mean microcharcoal surface area concentration curve (MCCsurf), (d) to (n) pollen group percentage curves. Pollen groups as in Figure 5.

https://doi.org/10.1016/j.yqres.2009.01.007 Published online by Cambridge University Press

development of other Ericaceae and semi-desert vegetation. This increase of fire regime contemporaneous with increasing fuel and a decrease of summer precipitation inferred from the decrease of *Calluna* would reflect environmental conditions favourable to fire propagation.

The decrease of fire regime in phase (c) at the end of HE4 is, at first sight, paradoxically associated with the development of mixed-wood forest (*Pinus*, *Picea* and Atlantic forests). The dominance of Cyperaceae and the new development of *Sphagnum* suggest again the development of mire. Although fire regime is expected to increase during this period as woody fuel is available, this wet environment might not promote fire spread, except at the very end of HE4 when *Picea* forest was more developed.

*Heinrich event 5.* As for HE4, three phases in the fire regime characterised HE5 (Fig. 6b). The decrease of fire regime in phase (a) occurs during a humid phase of low woody fuel (*Pinus* forest decline and *Calluna*-dominant vegetation). The relative low resolution of the pollen record during phase (b) precludes discussing the relationship between the increase of fire regime revealed by MCC and changes in forest cover and composition. The hypothesis of environmental conditions similar to HE4's phase (b) controlling this fire regime enhancement needs to be confirmed by higher resolution pollen analysis. The low fire regime in phase (c) is contemporaneous with *Pinus* forest and mire expansions. The record of *Pediastrum* at the very beginning of this phase suggests relative high amount of precipitation or strong snow melting, favouring the development of water-filled depressions (lakes, ponds) or lowland rivers (Batten, 1996) during this time. The following succession of Cyperaceae and *Sphagnum* suggests the progressive colonisation of these water-filled depressions.

During HE4 and 5, the progressive increase of annual SST recorded in phase (c) contemporaneous with the development of *Pinus* forest suggests warmer conditions than that of previous phases. Further, *Pinus* forest development during the middle and the last phases of HE4 and 5 would be indicative of a transition from a wet and/or cold (phase (a)) to a dry and/or warm climate (phase (b–c)) inferred from the establishment of trees on peatlands (see a synthesis in Linderholm and Leine, 2004). This drying and warming trend, observed during these two Heinrich events, has been also reported for the western Iberian margin and adjacent landmasses during the last phase of HE1, 2 and 4 (Naughton et al., 2007). In western France, the drying trend during the middle and last phase of HE 4 and 5 would lead to reduce fen landscapes and develop bog-dominated mire. Despite the relative drying and fuel availability, which would favour the increase of fire regime, moisture conditions are assumed to remain important enough in western France to limit propagation of fire at the end of these events. Finally, the increase of fire regime during phase (b), initially attributed to drought, could be also the result of an increase of frequency of lighting storms during this period, which could occur during an atmospheric reorganisation between phases (a) and (c).

*Heinrich event 6.* During HE6, we observe the development of *Picea* forest associated to the expansion of *Sphagnum* and *Pinus* populations, along with *Calluna* and Cyperaceae species, typical of the present-day vegetation of the Boreal region. Interestingly, HE6 is marked by a different vegetation pattern compared to HE5 and 4 because of the relative high percentages of *Pinus* over the entire event and the two slight declines of this tree. However, fire regime is also characterised by a three-phase structure (Fig. 6c). The first low fire regime, phase (a), is associated with *Pinus* forest decline. Phase (b) is characterised by a first strong increase of fire regime (b1) followed by a "plateau" (b2), which coincides with a relatively well developed *Pinus* and *Picea* forest associated with the expansion of *Sphagnum* growing in humid environments and semi-desert plants growing apart in drier soils. The decrease of fire regime at the end of HE6 (c) is associated with the maximum expansion of Cyperaceae and surprisingly with *Pinus* development.

As for HE4 and 5, the low fire regime during the first and last phases may be related to low fuel content and relative moist conditions limiting fire ignition and spread, respectively. The high fire regime during (b1) may be explained by the development of highly fire-sensitive Boreal forest system (Bergeron et al., 2004) associated with particularly dry climate as indicated by the strong development of semi-desert vegetation.

Beyond climatic conditions favourable to *Picea* and *Sphagnum* establishment during this period, high fire regime may have also contributed to the resulting vegetation assemblage. Permafrost forms in peatlands when mean annual temperature (MAT) is below 0°C and becomes continuous when MAT is under −6°C. However, Camill (2000) reports permafrost formation in Canadian boreal peatlands related to dense *Picea mariana* trees and *Sphagnum* dry peat, suggesting that cold temperature is not the unique factor involved in permafrost formation. Alternation between *Picea* and *Sphagnum* species in this region is triggered by fire. *Picea* trees diminish the solar radiation at the surface soil and permafrost begins to form. Fire alters *Picea* forest, the permafrost layer begins to melt and *Sphagnum* develops due to unfrozen conditions. Over time, peat accumulates and succession leads to favourable conditions for tree colonisation, which may promote permafrost formation.

We assume as a working hypothesis that *Picea* and *Sphagnum* grew together in western France during HE6. If we apply the present-day model of *P. mariana* in North America to *Picea* in western Europe, at longer time scale, the development of *Picea-Sphagnum* association during (b1) concomitant with high fire regime suggests that discontinuous permafrost occurred in western France during the transition MIS 4/MIS 3. Moreover, forest fires of this period were probably intense because the expansion of *Sphagnum* populations is favoured by high-temperature forest fires (Greisman, 2006). Paleosols testifying to short occurrence of permafrost have been detected in this region during the youngest HE2 and 1 (Bertran et al., 2008). In addition, evidence of permafrost formation during the HE6 time interval is suggested from growth cessation of the Grotte de Villars's speleothem located in southwestern France (Genty et al., 2003).

Fire regime stays at a high level during (b2) although this period is contemporaneous with woody fuel decrease (*Pinus* and *Picea* population decline) and increase in humidity (*Pediastrum* and Cyperaceae increase). However, *Pinus* forest decline was smaller than in HE4 and 5. At the same time, *Betula* forest-steppe expanded at the expenses of *Picea* (Fig. 5). This environmental succession might indicate thawing of permafrost under the onset of particular warming and drying trend, similar to that reported by Blyakharchuk and Sulerzhitsky (1999) for the western Siberia forest zone during the Holocene. This particular warming coincides with the start of obliquity increase (Fig. 5) and, therefore, enhancement of seasonal contrast at northern latitudes traced in our record by several well-marked GI characterised by the highest development of *Betula* associated with summer SST above 15°C. This particular warming could explain the maintenance of strong fire regime during (b2) likely resulted from particularly high summer temperatures, despite of the decline of *Pinus* and *Picea* forest.

## Conclusion

Microcharcoal and organic carbon analyses were applied to deep-sea core MD04-2845 recovered in the Bay of Biscay, at 45°N. Marine productivity variability revealed by organic carbon content parallels D–O climatic variability and is interpreted as a proxy of paleo-Navidad current strength. This current appears to have been reinforced during GI as the result of the prevailing negative NAO-like mode, and inversely during GS. Both GI and GS climatic situations were marked by dominant westerlies and microcharcoal concentration variation is independent of changes in fluvial sedimentary input, implying that D–

https://doi.org/10.1016/j.yqres.2009.01.007 Published online by Cambridge University Press

O microcharcoal concentration variability reflects fire regime variation in western France during the last glacial period.

The highest fire regimes are observed during GI related to high-fuel coniferous-mixed wooded vegetation. Decreasing fire regime is associated to fuel reduction in a steppe-dominated environment during HE and the other GS. This fire regime pattern is similar to that observed in southwestern Iberia for the same time period and supports a regional climatic control of fire regime, through biomass changes, in western Europe.

Contrary to the continuous low fire regime during HE in southwestern Iberia (Daniau et al., 2007), a three-phase structure characterises fire regime within HE6, 5 and 4 in western France. The highest fire regime episode is bracketed by two low fire regime phases. The first low fire regime phase is related to the *Pinus* forest decline and wet conditions, while the fire increase is contemporaneous with an afforestation. The late fire decrease is, paradoxically, associated with the maintenance of substantial woody fuel and dryer conditions than those of the previous phase. We explain this late decrease as the result of a new phase of mire expansion. This would indicate climatic conditions sufficiently moist to limit fire spread. During HE6, the strong relationship between the highest fire regime and the expansion of *Picea* and *Sphagnum* communities would reflect the formation of discontinuous permafrost.

## Acknowledgments

The work of A.-L. D. was supported by a BDI CNRS-région Aquitaine fellowship. This study was funded by the RESOLuTION (ESF-EUROCORES-EUROCLIMATE) and ARTEMIS projects. We gratefully acknowledge A. Landouar (LeicaMicrosystems) who provided useful assistance for LeicaQwin software language programming, B. Martin and E. Gonthier for advices and providing access to the slide polishing machine, H. Etcheber, H. Derriennic and A. Coynel for their introduction to organic carbon analysis, O. Ther for carbonate measurements, and J. Giraudeau for looking at the coccoliths of some slides of core MD04-2845. We also thank W. Fletcher, F. Naughton, S. Toucanne, C. Lopez-Martinez, J.-M Jouanneau, P. Bertran, C. Garcia-Soto and S. Harrison for their valuable comments on different sections of this manuscript. We also thank 2 anonymous reviewers and Boris Vannière as well as the editor for their valuable comments. This is Bordeaux 1 University, UMR-CNRS 5805 EPOC Contribution no. 1726.

## References

Allen, G.P., Castaing, P., 1977. Carte de répartition des sédiments superficiels sur le plateau continental du Golfe de Gascogne. Bull. Inst. Géol. Bassin d'Aquitaine 21, 255–261.

Andreae, M.O., Merlet, P., 2001. Emission of trace gases and aerosols from biomass burning. Global Biogeochemical Cycles 15, 955–966.

Bard, E., Rostek, F., Ménot-Combes, G., 2004. Radiocarbon calibration beyond 20,000 14C B.P. by means of planktonic foraminifera of the Iberian Margin. Quaternary Research 61, 204–214.

Batten, D.J., 1996. Palynofacies and palaeoenvironmental interpretation. In: Jansonius, J., McGregor, D.C. (Eds.), Palynology: Principles and Applications, 3. American Association of Stratigraphic Palynologists Foundation, pp. 1011–1064.

Beaufort, L., Heussner, S., 1999. Coccolithophorids on the continental slope of the Bay of Biscay — production, transport and contribution to mass fluxes. Deep-Sea Research II 46, 2147–2174.

Bergeron, Y., Gauthier, S., Flannigan, M., Kafka, V., 2004. Fire regimes at the transition between mixedwood and coniferous boreal forest in northwestern Quebec. Ecology 85, 1916–1932.

Bertran, P., Allenet, G., Gé, T., Naughton, F., Poirier, P., Sanchez Goni, M.F., 2008. Coversand and Pleistocene palaeosols in the Landes region, southwestern France. Journal of Quaternary Science, doi:10.1002/jqs.1220.

Blyakharchuk, T.A., Sulerzhitsky, L.D., 1999. Holocene vegetational and climatic changes in the forest zone of Western Siberia according to pollen records from the extrazonal palsa bog Bugristoye. The Holocene 9 (5), 621–628.

Boulter, M.C., 1994. An approach to a standard terminology for palynodebris. In: Traverse, A. (Ed.), Sedimentation of Organic Particles. Cambridge University Press, Cambridge, pp. 199–216.

Bradshaw, R.H.W., Tolonen, K., Tolonen, M., 1997. Holocene records of fire from the boreal and temperate zones of Europe. In: Clark, J.S., Cachier, H., Goldammer, H., Stocks, B. (Eds.), Sediment Records of Biomass Burning and Global Change. Springer-Verlag, Berlin, pp. 347–365.

Calvo, L., Tarrega, R., Luis, E., 2002. Regeneration patterns in a *Calluna vulgaris* heathland in the Cantabrian mountains (NW Spain): effect of burning, cutting and ploughing. Acta Oecologia 23, 81–90.

Camill, P., 2000. How much do local factors matter for predicting transient ecosytem dynamics? Suggestions from permafrost formation in boreal peatlands. Global Change Biology 6, 169–182.

Castaing, P., 1981. Le transfert à l'océan des suspensions estuariennes. Cas de la Gironde. Doct. es Sciences thesis, Université Bordeaux1.

Colas, F., 2003. Circulation et dispersion lagrangiennes en Atlantique Nord-Est. Thesis, Université de Bretagne Occidentale.

Combourieu Nebout, N., Turon, J.L., Zahn, R., Capotondi, L., Londeix, L., Pahnke, K., 2002. Enhanced aridity and atmospheric high-pressure stability over the western Mediterranean during the North Atlantic cold events of the past 50 ky. Geological Society of America 30, 863–866.

Crutzen, P.J., Heidt, L.E., Krasnec, J.P., Pollock, W.H., Seiler, W., 1979. Biomass burning as a source of atmospheric gases CO, H2, N2O, NO, CH3Cl and COS. Nature 282, 253–256.

Daniau, A.L., Sánchez Goñi, M.F., Beaufort, L., Laggoun-Défarge, F., Loutre, M.F., Duprat, J., 2007. Dansgaard–Oeschger climatic variability revealed by fire emissions in southwestern Iberia. Quaternary Science Reviews 26, 1369–1383.

Dupuis, H., Michel, D., Sottolichio, A., 2006. Wave climate evolution in the Bay of Biscay over two decades. Journal of Marine Systems 63, 105–114.

Durrieu de Madron, X., Castaing, P., Nyffeler, F., Courp, T., 1999. Slope transport of suspended particulate matter on the Aquitanian margin of the Bay of Biscay. Deep-Sea Research II 46, 2003–2027.

Enache, M.D., Cumming, B.F., 2006. Tracking recorded fires using charcoal morphology from the sedimentary sequence of Prosser Lake, British Columbia (Canada). Quaternary Research 65, 282–292.

European Commission, 2001. Forest Fires In Southern Europe. Environment and Geo-Information Unit report 1 (July).

Etcheber, H., Relexans, J.C., Beliard, M., Weber, O., Buscail, R., Heussner, S., 1999. Distribution and quality of sedimentary organic matter on the Aquitanian margin (Bay of Biscay). Deep-Sea Research II 46, 2249–2288.

Flückiger, J., Blunier, T., Stauffer, B., Chappellaz, J., Spahni, R., Kawamura, K., Schwander, J., Stocker, T.F., Dahl-Jensen, D., 2004. N2O and CH4 variations during the last glacial epoch: insight into global processes. Global Biogeochemical Cycles 18.

Froidefond, J.M., Castaing, P., Jouanneau, J.M., 1996. Distribution of suspended matter in a coastal upwelling area. Satellite data and in situ measurements. Journal of Marine Systems 8, 91–105.

Garcia-Soto, C., Pingree, R.D., Valdes, L., 2002. Navidad development in the southern Bay of Biscay: climate change and swoddy structure from remote sensing and in situ measurements. Journal of Geophysical Research 107 (C8), 3118.

Genty, D., Blamart, D., Ouahdi, R., Gilmour, M., Baker, A., Jouzel, J., Van-Exter, S., 2003. Precise dating of Dansgaard–Oeschger climate oscillations in western Europe from stalagmite data. Letters to Nature 421.

Greisman, A., 2006. Fire, forest and cultural landscape history during the last 11000 years in Småland — a case study at Stavsåkra. ESS Bulletin 4.

Heaps, N.S., 1980. A mechanism for local upwelling along the European continental slope. Oceanologica Acta 3, 449–454.

Hu, F.S., Brubaker, L.B., Gavin, D.G., Higuera, P.E., Lynch, J.A., Rupp, T.S., Tinner, W., 2006. How climate and vegetation influence the fire regime of the Alaskan boreal biome: the Holocene perspective. Mitigation and Adaptation Strategies for Global Change 11, 829–846C, doi:10.1007/s11027-005-9015-4.

Hughen, K.A., Baillie, M.G.L., Bard, E., Bayliss, A., Beck, J.W., Bertrand, C., Blackwell, P.G., Buck, C.E., Burr, G., Cutler, K.B., Damon, P.E., Edwards, R.L., Fairbanks, R.G., Friedrich, M., Guilderson, T.P., Kromer, B., McCormac, F.G., Manning, S., BronkRamsey, C., Reimer, P.J., Reimer, R.W., Remmele, S., Southon, J.R., Stuiver, M., Talamo, S., Taylor, F.W., van der Plicht, J., Weyhenmeyer, C.E., 2004. Marine04 marine radiocarbon age calibration, 0–26 cal kyr BP. Radiocarbon 46, 1059–1086.

Jouanneau, J.M., Weber, O., Cremer, M., Castaing, P., 1999. Fine-grained sediment budget on the continental margin of the Bay of Biscay. Deep-Sea Research II 46, 2205–2220.

Kennett, J.P., 1982. Marine Geology. Prentice-Hall, Englewood Cliffs, New Jersey.

Koutsikopoulos, C., le Cann, B., 1996. Physical processes and hydrological structures related to the Bay of Biscay anchovy. Scientia Marina 60 (2), 9–19.

Laitinen, J., Rehell, S., Oksanen, J., 2007. Community and species responses to water level fluctuations with reference to soil layers in different habitats of mid-boreal mire complexes. Plant Ecology, doi:10.1007/s11258-007-9271-3.

Laskar, J., Robutel, P., Joutel, F., Gastineau, M., Correia, A., Levrard, B., 2004. A long term numerical solution for the insolation quantities of the Earth. Astronomy and Astrophysics 428, 261–285.

Lazure, P., Jégou, A.M., 1998. 3D modelling of seasonal evolution of Loire and Gironde plumes on Biscay Bay continental shelf. Oceanologica Acta 21, 165–177.

Lericolais, G., Berné, S., Féniès, H., 2001. Seaward pinching out and internal stratigraphy of the Gironde incised valley on the shelf (Bay of Biscay). Marine Geology 175, 183–197.

Linderholm, H.W., Leine, M., 2004. An Assessment of twentieth century tree-cover changes on a southern Swedish peatland combining dendrochronology and aerial photograph analysis. Wetlands 24, 357–363.

Lobert, J.M., Scharffe, D.H., Hao, W.M., Crutzen, P.J., 1990. Importance of biomass burning in the atmospheric budgets of nitrogen-containing gases. Nature 346, 552–554.

Magri, D., 1994. Late-Quaternary changes of plant biomass as recorded by pollen-stratigraphical data: a discussion of the problem at Valle di Castiglione, Italy. Review of Palaeobotany and Palynology 81, 313–325.

McNamara, J.P., Siegel, D.I., Glaser, P.H., Beck, R.M., 1992. Hydrogeologic controls on peatland development in the Malloryville Wetland, New York (USA). Journal of Hydrology 140, 279–296.

Moreno, A., Cacho, I., Canals, M., Prins, M., Sánchez Goñi, M.F., Grimalt, J.O., Weltje, G.J., 2002. Saharan dust transport and high-latitude glacial climate variability: the Alboran sea record. Quaternary Research 58, 318–328.

Mouillot, F., Rambal, S., Joffre, R., 2002. Simulating climate change impacts on fire frequency and vegetation dynamics in a Mediterranean-type ecosystem. Global Change Biology 8, 423–437.

Myers, P.G., Haines, K., Rohling, E.J., 1998. Modeling the paleocirculation of the Mediterranean: the last glacial maximum and the Holocene with emphasis on the formation of sapropel S1. Paleoceanography 13, 586–606.

Naughton, F., Sánchez Goñi, M.F., Desprat, S., Turon, J.-L., Duprat, J., Malaizé, B., Joli, C., Cortijo, E., Drago, T., Freitas, M.C., 2007. Present-day and past (last 25000 years) marine pollen signal off western Iberia. Marine Micropaleontology 62, 91–114.

Ni, J., Harrison, S.P., Prentice, I.C., Kutzbach, J.E., Sitch, S., 2006. Impact of climate variability on present and Holocene vegetation: a model-based study. Ecological Modelling 191, 469–486.

Noël, H., 2001. Caractérisation et calibration des flux organiques sédimentaires dérivant du bassin versant et de la production aquatique (Annecy, le Petit lac). Rôles respectifs de l'Homme et du climat sur l'évolution des flux organiques au cours des 6000 dernières années. Ph. D. Thesis, Sciences de l'Univers, Pétrographie et Géochimie Organiques, Université d'Orléans, Orléans, France.

Ozenda, P., 1982. Les Végétaux Dans La Biosphère. Paris, Doin, p. 431.

Pailler, D., Bard, E., 2002. High frequency palaeoceanographic changes during the past 140,000 yr recorded by the organic matter in sediments of the Iberian margin. Palaeogeography, Palaeoclimatology, Palaeoecology 181, 431–452.

Petit, J.R., Jouzel, J., Raynaud, D., Barkov, N.I., Barnola, J.-M., Basile, I., Bender, M., Chappellaz, J., Davis, M., Delaygue, G., Delmotte, M., Kotlyakov, V.M., Legrand, M., Lipenkov, V.Y., Lorius, C., Pepin, L., Ritz, C., Saltzman, E., Stievenard, M., 1999. Climate and atmospheric history of the past 420,000 years from the Vostok ice core, Antarctica. Nature 399, 429–436.

Polunin, O., Walters, M., 1985. A Guide to the Vegetation of Britain and Europe. Oxford University Press, New York.

Power, M.J., Marlon, J., Ortiz, N., Bartlein, P.J., Harrison, S.P., Mayle, F.E., Ballouche, A., Bradshaw, R.H.W., Carcaillet, C., Cordova, C., Mooney, S., Moreno, P.I., Prentice, I.C., Thonicke, K., Tinner, W., Whitlock, C., Zhang, Y., Zhao, Y., Ali, A.A., Anderson, R.S., Beer, R., Behling, H., Briles, C., Brown, K.J., Brunelle, A., Bush, M., Camill, P., Chu, G.Q., Clark, J., Colombaroli, D., Connor, S., Daniau, A.-L., Daniels, M., Dodson, J., Doughty, E., Edwards, M.E., Finsinger, W., Foster, D., Frechette, J., Gaillard, M.J., Gavin, D.G., Gobet, E., Haberle, S., Hallett, D.J., Higuera, P., Hope, G., Horn, S., Inoue, J., Kaltenreider, P., Kennedy, L., Kong, Z.C., Larsen, C., Long, C.J., Lynch, J., Lynch, E.A., McGlone, M., Meeks, S., Mensing, S., Meyer, G., Minckley, T., Mohr, J., Nelson, D.M., New, J., Newnham, R., Noti, R., Oswald, W., Pierce, J., Richard, P.J.H., Rowe, C., Sánchez Goñi, M.F., Shuman, B.J., Takahara, H., Toney, J., Turney, C., Urrego-Sanchez, D.H., Umbanhowar, C., Vandergoes, M., Vanniere, B., Vescovi, E., Walsh, M., Wang, X., Williams, N., Wilmshurst, J., Zhang, J.H., 2007. Changes in fire regimes since the Last Glacial Maximum: an assessment based on a global synthesis and analysis of charcoal data. Climate Dynamics, doi:10.1007/s00382-007-0334-x.

Puillat, I., Lazure, P., Jégou, A.M., Lampert, L., Miller, P.I., 2004. Hydrographical variability on the French continental shelf in the Bay of Biscay, during the 1990s. Continental Shelf Research 24, 1143–1163.

Rixen, M., Beckers, J.-M., Levitus, S., Antonov, J., Boyer, T., Maillard, C., Fichaut, M., Balopoulos, E., Iona, S., Dooley, H., Garcia, M.J., Manca, B., A., G., Manzella, G., Mikhailov, N., Pinardi, N., Zavatarelli, M., the Medar Consortium, 2005. The Western Mediterranean Deep Water: a proxy for climate change. Geophysical Research Letters 32 NIL_47-NIL_50.

Rochefort, L., Campeau, S., Bugnon, J.-L., 2002. Does prolonged flooding prevent or enhance regeneration and growth of Sphagnum? Aquatic Botany 74, 327–341.

Ruch, P., Mirmand, M., Jouanneau, J.-M., Latouche, C., 1993. Sediment budget and transfer of suspended sediment from the Gironde estuary to Cap Ferret Canyon. Marine Geology 111, 109–119.

Sánchez Goñi, M.F., Cacho, I., Turon, J.-L., Guiot, J., Sierro, F.J., Peypouquet, J.P., Grimalt, J.O., Shackleton, N.J., 2002. Synchroneity between marine and terrestrial responses to millennial scale climatic variability during the last glacial period in the Mediterranean region. Climate Dynamics 19, 95–105.

Sánchez Goñi, M.F., Landais, A., Fletcher, W., Naughton, F., Desprat, S., Duprat, J., 2008. Contrasting impacts of Dansgaard–Oeschger events over a western European latitudinal transect modulated by orbital parameters. Quaternary Science Reviews 27, 1136–1151.

Serryn, P., 1994. Atlas Bordas Géographique. Hölzel, Paris.

Shackleton, N.J., et al., 2000. MD95-2042 Oxygen and Carbon Isotope Data. IGBP PAGES/World Data Center A for Paleoclimatology Data Contribution Series #2000-066. NOAA/NGDC Paleoclimatology Program. Boulder CO, USA.

Shackleton, N.J., Fairbanks, R.G., Chiu, T.-C., Parrenin, F., 2004. Absolute calibration of the Greenland time scale: implications for Antarctic time scales and for Δ14C. Quaternary Science Reviews 23, 1513–1522.

Stuiver, M., Reimer, P.J., 1993. Extended $^{14}C$ database and revised CALIB radiocarbon calibration program. Radiocarbon 35, 215–230.

Stuiver, M., Reimer, P.J., Reimer, R.W., 2005. CALIB 5.0. (www program and documentation).

Théry-Parisot, I., 1998. Economie du combustible et Paléoécologie en contexte glaciaire et périglaciaire, Paléolithique moyen et supérieur du sud de la France. Anthracologie, Experimentation, Taphonomie. Thesis, Université de Paris I Panthéon-Sorbonne.

Thonicke, K., Prentice, C.I., Hewitt, C., 2005. Modeling glacial–interglacial changes in global fire regimes and trace gas emissions. Global Biogeochemical Cycles 19, GB3008, doi:10.1029/2004GB002278.

Toucanne, S., Mulder, T., Schönfeld, J., Hanquiez, V., Gonthier, E., Duprat, J., Cremer, M., Zaragosi, S., 2007. Contourites of the Gulf of Cadiz: a high-resolution record of the paleocirculation of the Mediterranean outflow water during the last 50,000 years. Palaeogeography, Palaeoclimatology, Palaeoecology 246, 354–366.

Trigo, R.M., Osborn, T.J., Corte-Real, J.M., 2002. The North Atlantic Oscillation influence on Europe: climate impacts and associated physical mechanisms. Climate Research 20, 9–17.

Turon, J.-L., 1984. Le palynoplancton dans l'environnement actuel de l'Atlantique nord-oriental. Evolution climatique et hydrologique depuis le dernier maximum glaciaire. Mémoires de l'Institut de Géologie du bassin d'Aquitaine (17) Université de Bordeaux I, Bordeaux.

van Aardenne, J.A., Dentener, F.J., Oliver, J.G.J., Klein Goldewijk, C.G.M., Lelieveld, J., 2001. A 1 X 1 resolution data set of historical anthropogenic trace gas emissions for the period 1890–1990. Global Biogeochemical Cycles 15, 909–928.

Van der Werf, G.R., Randerson, J.T., Collatz, G.J., Giglio, L., Kasibhatla, S., Arellano, J.A.F., Olsen, S.C., Kasischke, E.S., 2004. Continental-scale partitioning of fire emissions during the 1997 to 2001 El Nino/La Nina Period. Science 303, 73–76.

Van Huissteden, J., Gibbard, P.L., Briant, R.M., 2001. Periglacial fluvial systems in northwest Europe during oxygen isotope stages 4 and 3. Quaternary International 79, 75–88.

Voelker, A.H.L., Lebreiro, S.M., Schönfeld, J., Cacho, I., Erlenkeuser, H., Abrantes, F., 2006. Mediterranean outflow strengthening during northern hemisphere coolings: a salt source for the glacial Atlantic? Earth and Planetary Science Letters 245, 39–55.